Research article

Journal of MASS SPECTROMETRY

Received: 23 October 2012 Revised: 27 November 2012 Accepted: 28 November 2012 Published online in Wiley Online Library

(wileyonlinelibrary.com) DOI 10.1002/jms.3149

Fatty acid neutral losses observed in tandem mass spectrometry with collision-induced dissociation allows regiochemical assignment of sulfoquinovosyl-diacylglycerols

Rosalia Zianni,[a] Giuliana Bianco,[b,c] Filomena Lelario,[c] Ilario Losito,[a,d] Francesco Palmisano[a,d] and Tommaso R.I. Cataldi[a,d]*

A full characterization of sulfoquinovosyldiacylglycerols (SQDGs) in the lipid extract of spinach leaves has been achieved using liquid chromatography/electrospray ionization-linear quadrupole ion trap mass spectrometry (MS). Low-energy collision-induced dissociation tandem MS (MS/MS) of the deprotonated species $[M-H]^-$ was exploited for a detailed study of sulfolipid fragmentation. Losses of neutral fatty acids from the acyl side chains (i.e. $[M-H-RCOOH]^-$) were found to prevail over ketene losses ($[M-H-R'CHCO]^-$) or carboxylates of long-chain fatty acids ($[RCOO]^-$), as expected for gas-phase acidity of SQDG ions. A new concerted mechanism for RCOOH elimination, based on a charge-remote fragmentation, is proposed. The preferential loss of a fatty acids molecule from the *sn*-1 position (i.e. $[M-H-R_1COOH]^-$) of the glycerol backbone, most likely due to kinetic control of the gas-phase fragmentation process, was exploited for the regiochemical assignment of the investigated sulfolipids. As a result, 24 SQDGs were detected and identified in the lipid extract of spinach leaves, their number and variety being unprecedented in the field of plant sulfolipids. Moreover, the prevailing presence of a palmitic acyl chain (16:0) on the glycerol *sn*-2 position of spinach SQDGs suggests a prokaryotic or chloroplastic path as the main route for their biosynthesis. Copyright © 2013 John Wiley & Sons, Ltd.

Additional supporting information may be found in the online version of this article.

Keywords: sulfoquinovosyldiacylglycerols; plant sulfolipids; tandem MS; collision-induced dissociation; spinach leaves; regiochemistry

Introduction

Although sharing the role of fundamental components of the hydrophobic barriers separating cells from their environment or subdividing their interiors into various compartments, plant lipids differ significantly from animal ones. The latter are represented mainly by phospholipids, like phosphatidylcholines, phosphatidylethanolamines, phosphatidylserines and sphingomyelins.[1] Lipids found in green plant cells are dominated by three characteristic glyceroglycolipids and one phospholipid, namely phosphatidylglycerol, representing the main polar lipid components of the thylakoid membrane of chloroplasts.[2] Among glyceroglycolipids, sulfolipids and galactolipids, species containing a sulfonic group and one (or two) galactose molecule(s), respectively, have been regarded as the predominant lipid components of the photosynthetic membrane in plants, algae and various bacteria.[3] In higher plants, monogalactosyl- (MGDG) and digalactosyl-diacylglycerols (DGDG) represent up to the 50 and 30 mol.%, respectively, of the thylakoid membrane of chloroplasts.[2] 1,2-diacyl-3-O-(6′-sulfo-α-D-quinovosyl)-*sn*-diacyl-glycerols (SQDGs) are relatively abundant sulfolipids specifically associated with photosynthetic membranes of higher plants, mosses, ferns, algae and most photosynthetic bacteria.[4] Their chemical structure is characterized by two non-polar fatty acyl chains, with various degrees of unsaturation, bonded to the glycerol backbone *sn*-1 and *sn*-2 positions, and a polar head group represented by a sulfoquinovose molecule (see Fig. 1).[5] In contrast to most naturally occurring sulfolipids, in which sulfur is involved in an ester (C-O-SO_3^-) linkage, SQDGs bear a sulfonic acid residue bonded to a carbon atom; sulfonic acids of this type are chemically very stable and strongly acidic in a wide pH range.[6]

Apart from their unusual chemical structure, SQDGs are quite intriguing lipids since their biological function is only partly understood. It is known that phosphate limitation results in a replacement of phospholipids by SQDGs in the thylakoid membrane of chloroplasts, required to maintain the overall amount of anionic lipids.[7] It has been also proposed that certain SQDGs

* *Correspondence to: Tommaso R. I. Cataldi, Dipartimento di Chimica, Università degli Studi di Bari Aldo Moro, Via E. Orabona, n° 4–70126 Bari, Italy. E-mail: tommaso.cataldi@uniba.it*

a *Dipartimento di Chimica, Università degli Studi di Bari Aldo Moro, Campus Universitario, Via E. Orabona, 4-70126 Bari, Italy*

b *Dipartimento di Scienze, Università degli Studi della Basilicata, Via dell'Ateneo Lucano, 10-85100 Potenza, Italy*

c *Centro Interdipartimentale Grandi Attrezzature Scientifiche - CIGAS, Università degli Studi della Basilicata, Via dell'Ateneo Lucano, 10-85100 Potenza, Italy*

d *Centro Interdipartimentale SMART, Università degli Studi di Bari Aldo Moro, Campus Universitario, Via E. Orabona, 4-70126 Bari, Italy*

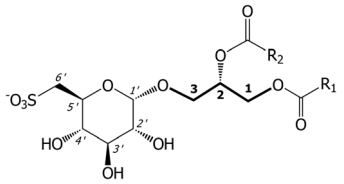

Figure 1. General structure of the deprotonated molecules of plant sulfolipids 1,2-diacyl-3-*O*-(6′-sulfo-α-D-quinovopyranosyl)-*sn*-glycerols (SQDGs).

are closely associated with protein complexes,[2] in which they are tightly bound, likely by electrostatic interactions, and participate either in catalytic activities or in maintaining the complexes in a functional conformation. In some cases, the interactions may be very strong, as suggested by the resistance of some SQDG molecules bound to chloroplast ATP synthase to exchange with other lipids.[8,9] Apparently, some SQDGs exhibit a remarkable antiviral activity, mainly against the human immunodeficiency virus (HIV-1),[10] and are clinically promising as antitumor and immunosuppressive agents.[11,12]

So far, mass spectrometry (MS) has played a key role in the identification of several SQDG species in bacterial[2,13,14] and algal[3,15–19] lipid extracts. On the other hand, MS investigations of SQDGs in plant matrices are quite limited in number and, to the best of our knowledge, almost exclusively related to the identification of SQDGs in *Arabidopsis* leaves extracts by electrospray ionization (ESI)/MS/MS.[20–22] The regiochemical characterization of SQDG species, i.e. the location of their acyl chains on the *sn*-1 and *sn*-2 positions of the glycerol backbone, has been attempted in some of the cited investigations. In particular, the preferential neutral loss of the *sn*-1-linked acyl chain, as the corresponding fatty acid, during low-energy (collision-induced) CID MS/MS analysis of SQDGs in an extract of the marine chloromonad *Heterosigma carterae* was explicitly invoked by Keusgen *et al.*[15] for the purpose of regiochemical assignment, although no mechanistic explanation was provided. In other studies, the interpretation of regiochemically related fragmentations of SQDGs appears to be controversial.[16–18]

In order to clarify these aspects, a systematic characterization of sulfolipids extracted from spinach leaves has been undertaken using a reversed-phase liquid chromatography (RPLC) separation and ESI/MS with a linear quadrupole ion trap (LTQ). Interestingly, the prevalence of neutral fatty acid losses from the *sn*-1 positions of the glycerol backbone during CID MS/MS experiments has been exploited for the systematic regiochemical assignment of SQDGs. A new concerted mechanism for these neutral losses, based on a charge-remote fragmentation, has been invoked. In the following, R_1 and R_2 notations stand for the acyl chains on the glycerol backbone *sn*-1 and *sn*-2 positions, respectively.

Experimental

Chemicals

LC/MS-grade methanol and acetonitrile and HPLC-grade isopropyl alcohol were purchased from Carlo Erba (Milan, Italy); ACS-reagent grade ammonium hydroxide was purchased from Sigma-Aldrich (Milan, Italy). Ultra-pure water was produced using a Milli-Q RG system from Millipore (Bedford, MA, USA).

Plant sulfolipids mixture

A mixture of SQDGs extracted from spinach leaves, purchased from Lipid Products (Redhill, UK) and stored in chloroform stabilized with 3% methanol, was used as stock solution. A working solution at 10 μg/ml concentration was obtained by subsequent dilutions with methanol of the stock solution and then analyzed by LC/MS.

LC/MS

RP separations of SQDGs were performed using a Surveyor LC System (Thermo Scientific, Bremen, Germany) coupled to a Supelco Discovery C18 (Sigma-Aldrich, Milan, Italy) column (250 × 4.6 mm, 5 μm particle packing). LC runs were performed at ambient temperature (21 ± 2 °C) and at a flow rate of 1.0 ml/min; the column effluent was split to allow 200 μl/min to enter the ESI source. A binary mobile phase composed of water (solvent A) and acetonitrile (solvent B), both containing 5% (v/v) isopropyl alcohol and 15 mM ammonium hydroxide, was used.[17] The elution program was from 50 to 92 % B in 5 min, isocratic for 20 min, 100 % B in 2 min, isocratic for 10 min then back to 50 % B in 3 min, followed by 5 min equilibration time.

The linear ion trap spectrometer embedded in a LTQ-FT hybrid linear trap/7-T ICR mass spectrometer (Thermo Scientific), coupled to the described HPLC system by a ESI interface, was used for MS analyses. As for ESI parameters, the spray voltage was +5.0 kV, producing a spray current of approximately 3 μA, the temperature of the ion transfer tube was 330 °C, and the applied voltage was −10 V. The sheath gas (N_2) flow rate used was 60 (arbitrary units). Negative ion full-scan mass spectra were acquired, as profile data, in the *m/z* range 150–1000. External calibration of the instrument was performed using the standard calibration mixture provided by the manufacturer. CID-MS/MS and -MS^3 experiments on monoisotopically isolated precursor ions were performed with a collisional energy (CE) comprised between 25% and 35% of the maximum available value, using an activation time of 10 ms and an activation *q* value of 0.25. Data acquisition and analysis were accomplished using the Xcalibur software package (version 2.0 SR1 Thermo Electron). All the spectra reported are the average of 15–25 scans. The chromatographic raw data were imported, elaborated and plotted by SigmaPlot 9.0 (Systat Software, Inc., London, UK). ChemDraw Pro 8.0.3 (CambridgeSoft Corporation, Cambridge, MA, USA) was employed to draw chemical structures.

Results and discussion

LC/ESI-MS analysis of an extract of plant sulfolipids

A preliminary survey of LC/ESI-MS data on SQDGs was accomplished by ion current extraction. Specifically, eXtracted Ion Chromatograms (XICs) obtained using a ±0.2 *m/z* window, were retrieved for *m/z* ratios expected for the $[M-H]^-$ ions of putative sulfolipid species. For the sake of clarity, three cumulative XICs, referring to species bearing a total of 36, 34 and 32 carbon atoms on their acyl chains, respectively, are reported in panels (**a**), (**b**) and (**c**) of **Fig. 2.** Twenty-four likely SQDGs, including six couples of isobaric compounds, were distinguished. Assuming a similar ESI efficiency, 10 species, *viz.* those with $[M-H]^-$ ions at *m/z* 837.5, 839.5, 841.5 and 843.5 (see panel **a** in **Fig. 2**), 815.5, 817.5, 819.5 and 821.5 (panel **b**), 787.5 and 793.5 (panel **c**), were

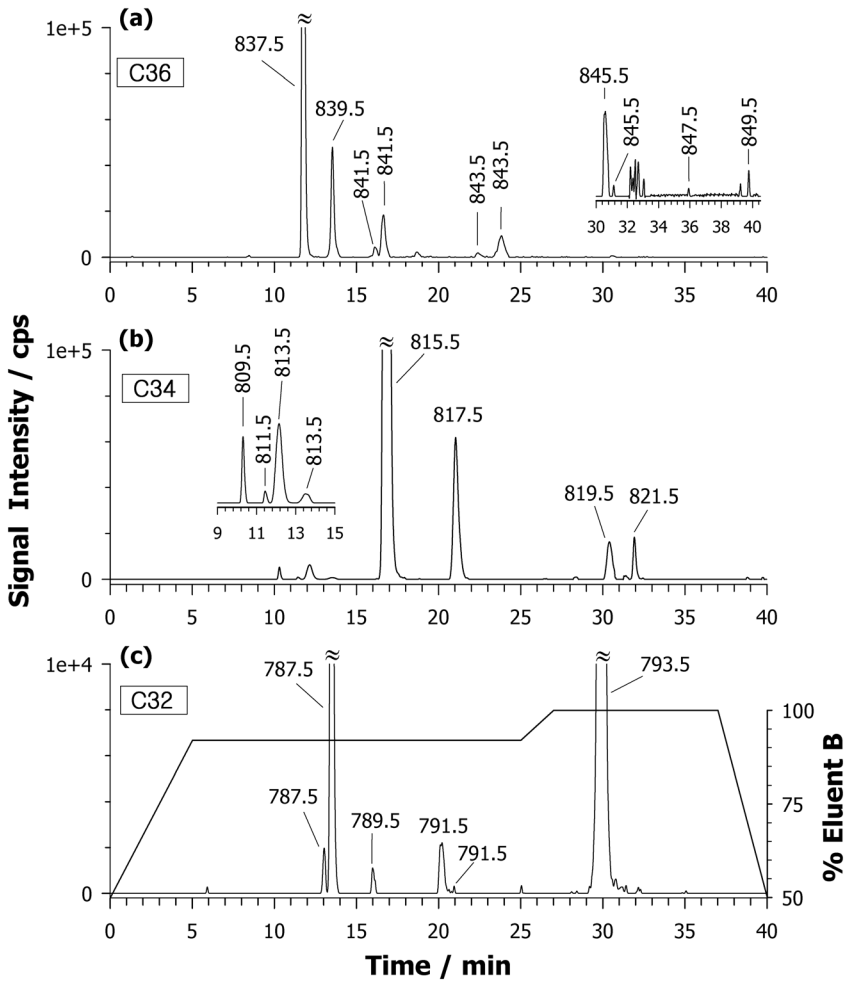

Figure 2. Extracted ion chromatograms (XICs) retrieved from the LC/ESI MS full scan (*m/z* 200–1000) chromatogram of a mixture of SQDGs (10 μg ml^{-1}) extracted from spinach leaves: (a) ions at *m/z* 837.5, 839.5, 841.5, 843.5, 845.5, 847.5 and 849.5; (b) ions at *m/z* 809.5, 811.5, 813.5, 815.5, 817.5, 819.5 and 821.5; (c) ions at *m/z* 787.5, 789.5, 791.5 and 793.5. In each panel, the total number of carbon atoms on the two acyl chains of SQDG species is highlighted. The gradient profile is superimposed on plot (c).

found as the major sulfolipids in the analyzed extract. The chromatographic step allowed the separation of structural isomers (*vide infra*), corresponding to different distributions of carbon atoms and/or unsaturations between the two acyl chains, and regioisomers, characterized by a different positioning of the same couple of acyl chains on the *sn*-1 and *sn*-2 positions of the glycerol backbone. Retention times of RPLC separations and MS data of all SQDGs are summarized in the second and third columns of **Table 1**, respectively.

Identification of the SQDG acyl chains by CID-MS/MS

An example of tandem MS spectrum for the $[M-H]^-$ ion (M + 0 isotopologue) of a possible SQDG (*m/z* 793.5) is reported in **Fig. 3**. Apart from the well-known class-diagnostic fragment ion at *m/z* 225.1[14,20] (see the left inset), the most prominent product ion was found at *m/z* 537.4, representing the neutral loss of a palmitic acid (16:0) molecule ($[M-H-C_{15}H_{31}COOH]^-$). This loss is clearly prevailing over the ketene (K) loss, leading to the $[M-H-C_{14}H_{29}CH=C=O]^-$ ion (*m/z* 555.4). Moreover, a relatively low intensity peak was detected at *m/z* 255.2, which can be assigned to the palmitate anion (i.e. $[C_{15}H_{31}COO]^-$). As no other significant signals are detected in the MS/MS spectrum, these findings definitely confirm that the $[M-H]^-$ ion at *m/z* 793.5 identifies a 16:0/16:0 SQDG.

The prevalence of neutral fatty acid losses among fragmentation routes achieved by CID-MS/MS of SQDG deprotonated molecules $[M-H]^-$ was confirmed for all the species detected in the analyzed sample (*vide infra*). Most of them are characterized by the presence of different acyl chains on the *sn*-1 and *sn*-2 positions of the glycerol backbone (**Table 1**). An example of MS/MS spectrum for this type of SQDGs is shown in **Fig. 4** for a precursor ion at *m/z* 815.5, corresponding to a species bearing 34 carbon atoms belonging to the two acyl chains and a total of three unsaturations on the same acyl chains (i.e. a 34:3 SQDG). Besides the product ion at *m/z* 225.1, major peaks are observed at *m/z* 537.5 and 559.5 and minor ones at *m/z* 255.2, 277.4, 555.5 and 577.5. The last six *m/z* ratios correspond to three couples of product ions, each related to one of the fragmentations already discussed for the 16:0/16:0 SQDG (see the assignments in **Fig. 4**), and allow to identify the two acyl chains as 18:3 (i.e. presumably linolenic) and 16:0 (i.e. palmitic) ones (see the right inset in **Fig. 4**). Also, in this case, product ions deriving from ketene losses (i.e. $[M-H-K_1]^-$ and $[M-H-K_2]^-$) are significantly less abundant than those corresponding to neutral losses of fatty acids, i.e. $[M-H-R_1COOH]^-$ and $[M-H-R_2COOH]^-$. Interestingly, the *m/z* ratios of side chain-related product ions, especially those resulting from

Table 1. Retention times, *m/z* ratios of deprotonated molecules and regiochemical composition (*sn*-1/*sn*-2) of 24 SQDG species identified in a lipid extract of spinach leaves by LC/ESI MS/MS measurements in negative ion mode. The last column reports the intensity ratio A_1/A_2 of two diagnostics product ions[a]

n SQDG[b]	Retention time (min)	$[M-H]^-$ (*m/z*)	*sn*-1/*sn*-2[c]	$(A_1/A_2) \pm SD$ [d]
1)	10.3	809.5	18:3/16:3	1.32 ± 0.13
2)	11.4	811.5	16:2/18:3	2.48 ± 0.18
3)	11.8	837.5	18:3/18:3	NA
4)	12.2	813.5	16:1/18:3	1.51 ± 0.12
5)	13.0	787.5	14:0/18:3	2.42 ± 0.22
6)	13.3	813.5	18:3/16:1	1.61 ± 0.12
7)	13.5	839.5	18:2/18:3	2.07 ± 0.08
8)	13.5	787.5	16:3/16:0	3.14 ± 0.07
9)	16.0	789.5	16:2/16:0	2.95 ± 0.11
10)	16.1	841.5	18:2/18:2	NA
11)	16.7	841.5	18:1/18:3	1.82 ± 0.07
12)	16.8	815.5	18:3/16:0	2.04 ± 0.08
13)	20.2	791.5	16:1/16:0	1.22 ± 0.12
14)	20.9	791.5	16:0/16:1	1.68 ± 0.18
15)	21.0	817.5	18:2/16:0	2.21 ± 0.09
16)	22.4	843.5	18:3/18:0	1.58 ± 0.12
17)	23.9	843.5	18:0/18:3	1.77 ± 0.18
18)	29.9	793.3	16:0/16:0	NA
19)	30.4	819.5	18:1/16:0	2.25 ± 0.08
20)	30.6	845.5	18:1/18:1	NA
21)	31.1	845.5	18:0/18:2	1.22 ± 0.12
22)	31.9	821.5	18:0/16:0	2.48 ± 0.17
23)	36.0	847.5	20:1/16:0	2.78 ± 0.23
24)	39.7	849.5	20:0/16:0	1.87 ± 0.22

[a]See experimental conditions. [b] Sulfolipids listed according to their elution order. [c] Regiochemistry of fatty acids assigned on the basis of CID tandem MS. [d]A_1 and A_2 represent the signal intensity of peaks corresponding to $[M-H-R_1COOH]^-$ and $[M-H-R_2COOH]^-$ fragments, respectively. SD is the standard deviation evaluated over three MS/MS spectra. NA, not applicable.

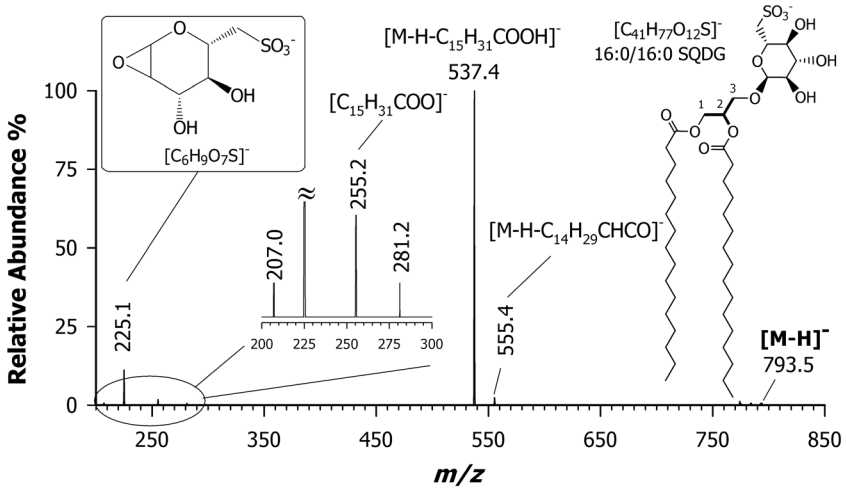

Figure 3. CID MS/MS product ion spectrum obtained by LC/ESI in negative ion mode for the $[M-H]^-$ ion (monoisotopic) of the 16:0/16:0 SQDG (*m/z* 793.5), fragmented at 35% collision energy. The chemical structure of the precursor ion and of the product ion at *m/z* 225.1 (see ref.[13]) are illustrated in the right and left insets, respectively. The presence of minor product ions is emphasized in the vertically expanded region.

fatty acid losses, enabled an immediate distinction between structurally isomeric SQDGs. In the specific case of the *m/z* 815.5 ion, other acyl chain combinations compatible with a 34:3 composition, such as 20:3/14:0, 18:2/16:1, etc., can be easily discarded. The assignment of double bond(s) location in the unsaturated fatty acid substituents was not performed in this study; in all SQDG structures, the location of double bond(s) were assigned according to Takahashi *et al.*[23]

Likewise, couples of isobaric/isomeric SQDGs characterized by different combinations of acyl chains were found at other *m/z* ratios. As an example, CID MS/MS spectra obtained for two species whose $[M-H]^-$ ions exhibit *m/z* 787.5 (i.e. SQDGs 5 and 8 in Table 1) are compared in **Fig. 5**. The CID fragmentations of these two isobaric sulfolipids, eluted at slightly different retention times, *viz.* 13.0 and 13.5 min, may be related to isomeric compounds

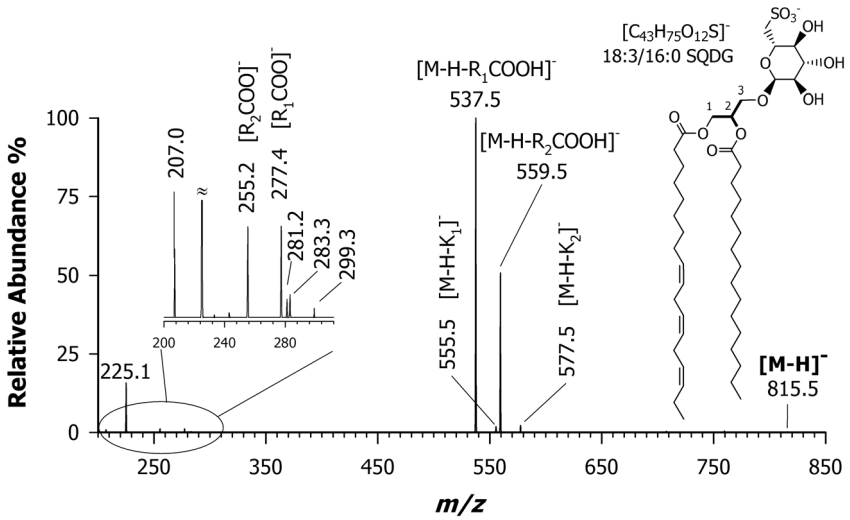

Figure 4. CID MS/MS product ion spectrum obtained by LC/ESI in negative ion mode for the $[M-H]^-$ ion of the 18:3/16:0 SQDG (*m/z* 815.5), fragmented at 35% collision energy. The chemical structure of the precursor ion is reported in the right inset. The signals related to minor product ions are discernible in the vertically expanded region. $[M-H-K_i]^-$ ions correspond to product ions arising from ketene losses.

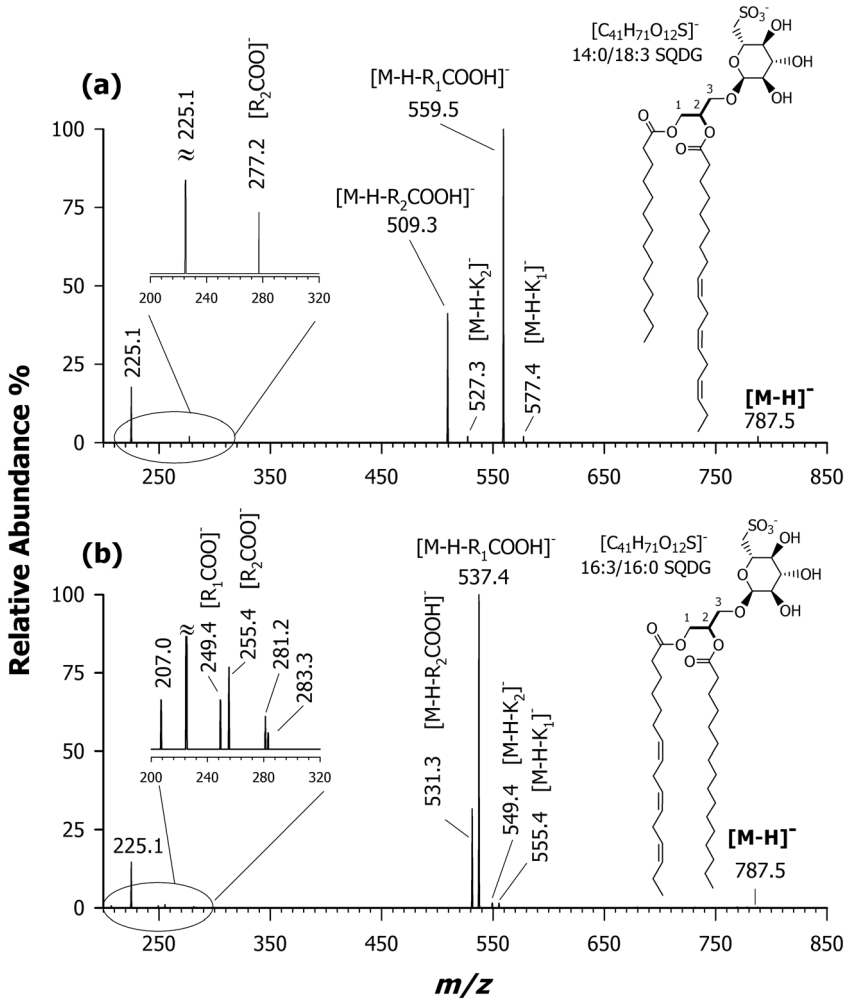

Figure 5. CID MS/MS product ion spectra of two isobaric SQDGs, 14:0/18:3 (a) and 16:3/16:0 (b), whose $[M-H]^-$ ions had *m/z* 787.5 and that were eluted at retention times of 13.0 and 13.5 min, respectively. The left insets provide expanded views of peaks related to long chain carboxylate anion, as $[R_1COO]^-$ and $[R_2COO]^-$, along with some minor product ions (panel b) discussed in the text. The molecular structures reported are based on the fatty acids losses interpretation (see text for details).

such as 14:0/18:3 (panel a) and 16:3/16:0 (panel b) acyl chains, respectively (see the suggested molecular structures in **Fig. 5**).

Most importantly the predominance of fatty acid losses over ketene ones and carboxylate anions generation, observed systematically during the present investigation, may be inferred from most of the MS/MS spectra previously reported for SQDGs[3,15–18] and is well consistent with the acidity of SQDG ions in the gas phase. Indeed, the same behavior has been reported for other glycerophospholipids whose gas-phase molecules are easily deprotonated $[M-H]^-$, such as glycerophosphatidic acids (PAs) and phosphatidyl-inositols (PIs).[24] Moreover, the prevalence of fatty acid losses has been observed also for MGDGs and DGDGs, when analyzed as positive ions (usually as adducts with Li^+, Na^+ or NH_4^+ ions) using quadrupole ion trap[25] or linear ion trap[26] analyzers. The cited investigations also suggest that the exact location of each side chain on the glycerol backbone can be retrieved from low-energy CID MS/MS spectra of glycerol(phospho)lipids by interpreting fatty acid losses or ketene ones, if these prevail, as in the case of precursor ions of positive-ion adducts.[24] In spite of the several MS/MS investigations already reported,[2,13–18] this aspect appears still controversial in the case of SQDG species, perhaps because regiochemically defined standards are hard to obtain. Nonetheless, a survey of the few low-energy CID MS/MS data already reported for SQDGs whose regiochemistry had been independently and reliably ascertained (e.g. exploiting the regiospecific hydrolysis of the ester linkage involving the *sn*-1 acyl chain, enabled by the Lipase XI from *Rhizopus arrizhus*[27,28]) indicates that the fatty acid loss from the *sn*-1 position is generally favored.[15,16,18] A comparison with the mechanisms reported for the fatty acid losses from other glycerophospholipid classes may help in clarifying this point.

Fatty acid losses from glycerol(phospho)lipids: mechanistic aspects

The mechanisms underlying the loss of fatty acids from the acyl chains of glycerophospholipids have been discussed in several instances.[24,26,29] When negatively charged precursor ions are considered (e.g. in the case of PAs and PIs) the phosphate negative charge is supposed to be directly involved in proton abstraction from either the *sn*-2 (methynic proton) or *sn*-1 (methylenic protons) positions of the glycerol backbone, leading to fatty acid loss from the corresponding position. Starting from sterical considerations, the prevalence of fatty acid loss from the *sn*-2 position was suggested by Hsu and Turk[24] and confirmed by experimental data. However, when the $[M-H]^-$ ions of SQDGs are considered, the negative charge, located on the sulphonic group, does not appear to be close enough to the fragmentation site to make the above cited mechanism applicable.

Under low-energy CID conditions, sodium[25] and lithium[26] adducts of MGDGs and DGDGs, representing two interesting examples of positively charged glycolipids, exhibit the preferential loss of the *sn*-1 chain as a neutral fatty acid. Tatituri *et al.*[26] proposed a complex pathway to explain the fatty acid losses from the lithium adducts of MGDGs and DGDGs, involving the transfer of a methylenic hydrogen from the α−carbon atom of one of the acyl chains to the carbonylic oxygen of the other acyl chain, finally detached as a carboxylic acid. Thus, the prevalence of fatty acid loss from the *sn*-1 position was justified with the observation that the transfer of α-hydrogens located on the *sn*-2 chain is favored over that of the corresponding hydrogens on the *sn*-1 chain. This consideration arises from a previous study focusing on the phosphocholine loss from PC specifically deuterated on the α-hydrogens of the acyl chains (d_{27}-14:0/d_{26}-14:0-PC, d_{27}-14:0/14:0-PC and 14:0/d_{27}-14:0-PC).[29] Very recently, in order to explain the fatty acid losses from SQDGs, Reid and coworkers[14] have proposed a 1,3 *cis* elimination, implying the transfer of glycerol methylenic or methynic hydrogens towards esteric, instead of carbonylic, oxygen atoms of the acyl chains, albeit no explanation of the prevalence of R_1COOH losses has been provided.

However, if an alternative conformation is assumed for the acyl chains with respect to the glycerol backbone, a simpler mechanism can be proposed to explain the neutral losses of fatty acids from SQDGs and, more generally, from other glycolipids, like MGDGs and DGDG, in which no assistance by a negative charge is inherently invoked for that fragmentation. As depicted in Scheme 1, a concerted mechanism for RCOOH elimination can be considered as a typical *charge-remote fragmentation* (CRF), in which the charged site is supposed to be remote from the site involved in the fragmentation process. Such a process is similar to gas-phase thermal reactions of neutral long-chain molecules but occurring in even electron precursor ions.[30,31] Indeed, the loss of fatty acid chains, along with several other fragmentations observed during FAB-MS/MS measurements on the $[M+Na]^+$ ions of SQDGs isolated from wild-type cyanobacterium *Synechocystis*,[2]

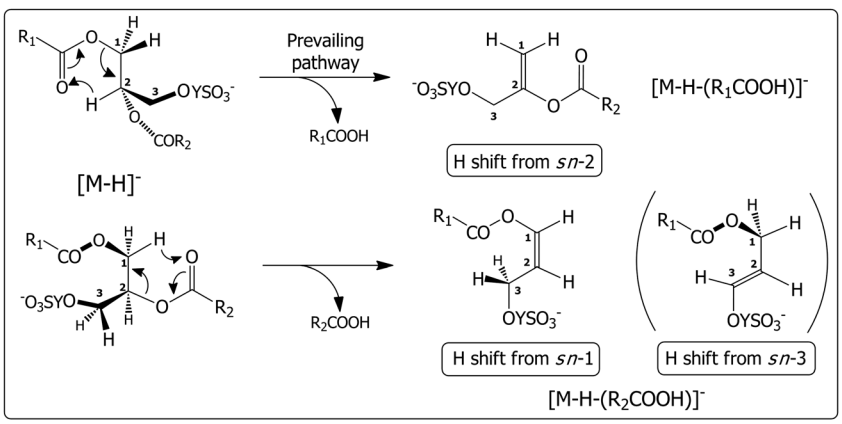

Scheme 1. Concerted mechanism via thermal reactions of the charge-remote type proposed to describe the elimination of neutral fatty acids from SQDG species under ESI/CID MS/MS. Bold numbers represent the stereospecific numbering of the glycerol backbone. The route involving an H transfer from the *sn*-3 carbon of glycerol is not reported for the sake of brevity. Y represents the sulfoquinovosyl moiety.

Journal of MASS SPECTROMETRY

has been included among CRF processes occurring on glycolipids (see Scheme 2 in Ref.[31]

It is worth noting that, whereas one of the four methylene hydrogens linked to glycerol *sn*-1 and *sn*-3 carbon atoms could be transferred to the carbonyl oxygen on the *sn*-2-linked acyl chain, leading to a R_2COOH loss, only the single methynic hydrogen on the *sn*-2 carbon atom could be transferred to the carbonyl oxygen of the *sn*-1-linked acyl chain, leading to a neutral loss of R_1COOH. Accordingly, one would expect the R_2COOH loss to be favored by a 4:1 factor over the R_1COOH one. Steric hindrance-related and energetic considerations could explain why this prediction is not confirmed by the experimental MS/MS data on SQDGs with known regiochemistry, showing the prevalence of the fatty acid loss from the *sn*-1 position. Specifically, the transfer of one of the two hydrogens linked to the *sn*-3 position of glycerol towards the carbonylic oxygen of the *sn*-2-linked acyl chain (not shown in **Scheme 1**) could be hindered by the proximity of the sulfoquinovosyl moiety. Moreover, the transfer of one of the four methylenic hydrogens could be energetically unfavorable with respect to that of the single methynic hydrogen, due to the different nature of the saturated carbon atoms they are linked to, i.e. secondary and tertiary, respectively. Additionally, there is the possibility that in the case of R_1COOH loss, the most stable $[M-H-R_1COOH]^-$ product ion could arise from a gas-phase decomposition process under kinetic rather than thermodynamic control.

Isotopically labeled analogues of SQDG species, bearing different acyl chains on the *sn*-1 and *sn*-2 positions and characterized by the presence of deuterium atoms in place of specific hydrogen atoms linked either to the glycerol backbone or to the acyl chains, would be very useful in ascertaining which hydrogen atoms are really involved in the neutral losses of fatty acids. However, as already demonstrated by Reid *et al.*,[14] only the H atoms of the OH groups on the sulfoquinovosylic ring can be exchanged with D in the case of SQDGs, thus the H/D exchange cannot be exploited for the elucidation of the fatty acid loss mechanism.

Regiochemistry of SQDGs in spinach leaves

Starting from the mechanistic considerations made in the previous section, the location of acyl chains for each of the 24 SQDGs detected in the spinach extract was accomplished by evaluating the relative abundance ratios of diagnostic product ions $[M-H-R_1COOH]^-$ and $[M-H-R_2COOH]^-$, in the following referred to as A_1 and A_2, respectively. An important point to remember is that the fatty acid loss was the prevailing fragmentation even when lower values of CE were applied to SQDGs precursor ions. The calculated A_1/A_2 ratios obtained with a CE of 35% are summarized in Table 1; values greater than unity were observed systematically, thus enabling the regiochemical assignment. Most interestingly, couples of chromatographically separated regioisomeric SQDG species could

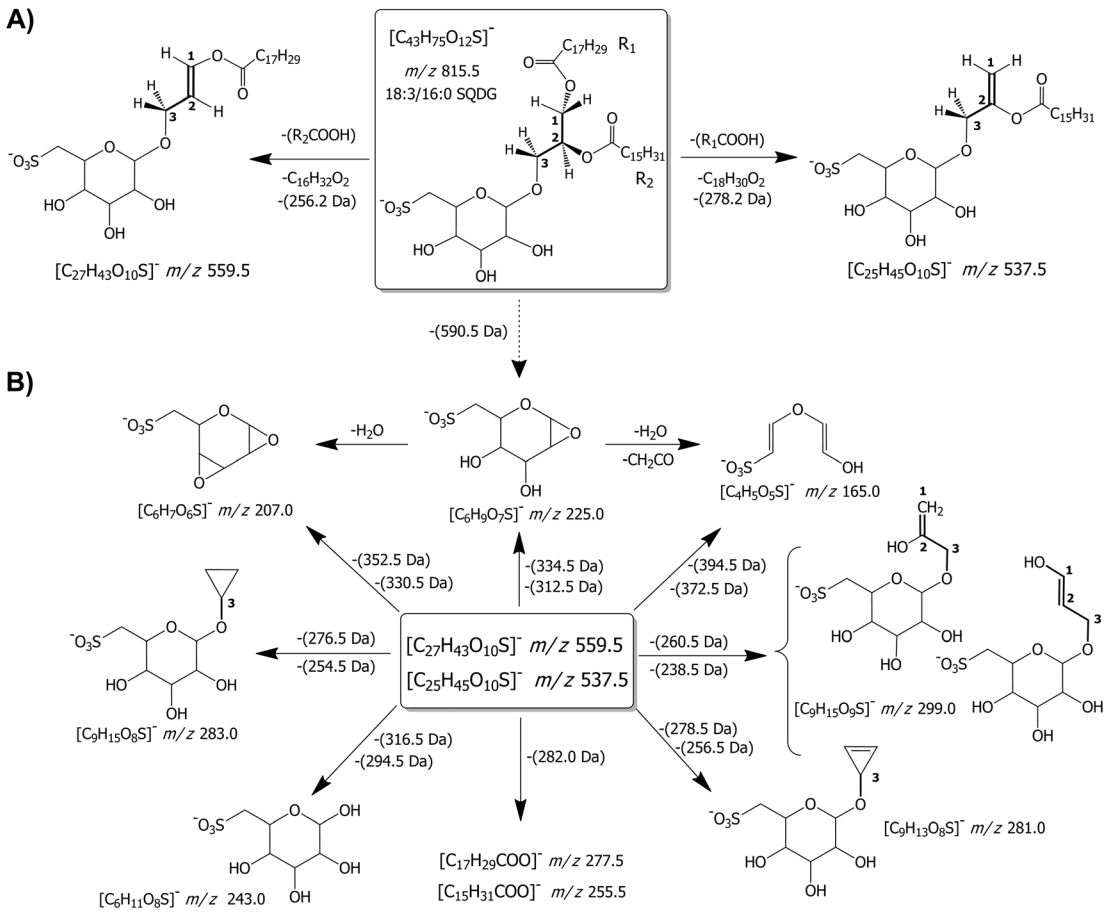

Scheme 2. Fragmentation reactions proposed to describe (A) the most prominent product ions $[M-H-R_1COOH]^-$ and $[M-H-R_2COOH]^-$ from SQDGs in ESI/CID MS/MS measurements in a linear quadrupole trap and (B) the formation of lighter ions from $[M-H-R_1COOH]^-$ and $[M-H-R_2COOH]^-$ in ESI/CID MS^3 experiments. The fragmentation pathways for the MS/MS precursor ion for the 18:3/16:0 SQDG, at *m/z* 815.5, are shown as an example. The dashed arrow represents the direct formation of the class-diagnostic fragment at *m/z* 225.0. The chemical structures of the *m/z* 281.0 and 283.0 ions are only tentatively assigned.

be distinguished by simply evaluating the A_1/A_2 ratios. An example is represented by the two isobaric SQDGs (numbered as 4 and 6 in **Table 1**) bearing 18:3 and 16:1 acyl chains (*m/z* 813.5), whose MS/MS spectra are compared in **Fig. 6**. These sulfolipids are minor components in the analyzed mixture; nonetheless, their CID-MS/MS spectra clearly show the usual predominance of product ions $[M-H-R_1COOH]^-$ and $[M-H-R_2COOH]^-$. Moreover, as a result of the inversed position of the two acyl chains, a clear inversion of the relative intensity of peaks at *m/z* 535.5 and 559.5 is observed. This finding confirms that fatty acid loss by CID-MS/MS of SQDG species is basically driven by the specific detachment site on the precursor ion (with *sn*-1 always preferred over *sn*-2) rather than by the nature of the detached fatty acids. As already mentioned, the predominance of kinetic effects over thermodynamic ones can be then inferred for this fragmentation pathway. Further examples of SQDG species regiochemically characterized by CID-MS/MS (i.e. 18:2/18:3, at *m/z* 839.5, and 18:0/18:3, at *m/z* 843.5) are given in the Supporting Information (Figs. S1 and S2).

CID-MS^3 analyses

After completing the regiochemical assignments, MS^3 experiments were accomplished on diagnostic product ions $[M-H-R_1COOH]^-$ and $[M-H-R_2COOH]^-$ of some SQDGs, in order to extend their fragmentation pathways. The product ion spectra of *m/z* 559.5 and 537.3 ions, in turn corresponding to the main product ions of the 18:3/16:0 SQDG (*m/z* 815.5), are shown in **Fig. 7**. In both cases, the base peak is the already cited *m/z* 225.1 ion, for which a structure bearing an epoxydic bridge between carbon 1 and 2 of the quinovosylic ring has been recently proposed by Reid and coworkers, after H/D exchange experiments.[14]

The only significant difference between spectra compared in **Fig. 7** is the presence of peaks at *m/z* 277.2 and 255.2, arising from precursor ions at *m/z* 559.5 and 537.5, respectively, and easily assigned to 18:3 $[C_{18}H_{29}O_2]^-$ (linolenic) and 16:0 $[C_{16}H_{31}O_2]^-$ (palmitic) carboxylate anions (see **Scheme 2**, panel A). Among minor product ions, shared by the two MS^3 spectra, those at *m/z* 299.1 and 281.2 are due to losses, as ketene or carboxylic acid, respectively, of the acyl chain remaining in the precursor ion, as shown in **Scheme 2** (panel B). The proposed chemical structures for each fragment have been deduced from logical fragmentation pathways and reflect the chemical compositions correctly. However, the chemical structures presented in the fragmentation pattern cannot be unequivocally verified. For example, the proposed structures for the *m/z* 281.0 and 283 ions, resulting from the loss of the remaining acyl chain as a different molecule,

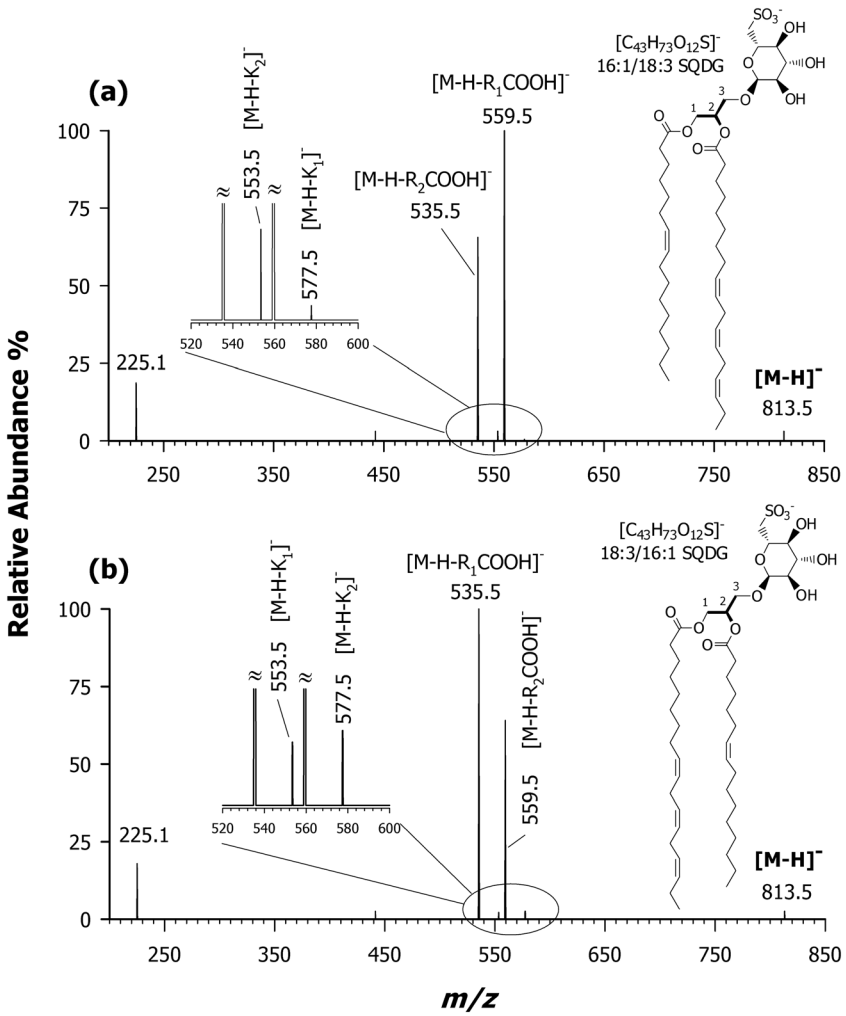

Figure 6. CID MS/MS product ion spectra of two regioisomeric SQDGs, 16:1/18:3 (a) and 18:3/16:1 (b), having *m/z* 813.5 and eluted at retention times of 12.2 and 13.5 min, respectively. In the insets, vertical expansions of spectra are shown for *m/z* intervals including ions generated by loss of ketenes, K_1 and K_2. The molecular structures reported are based on the fatty-acid-molecule losses interpretation (see text for details).

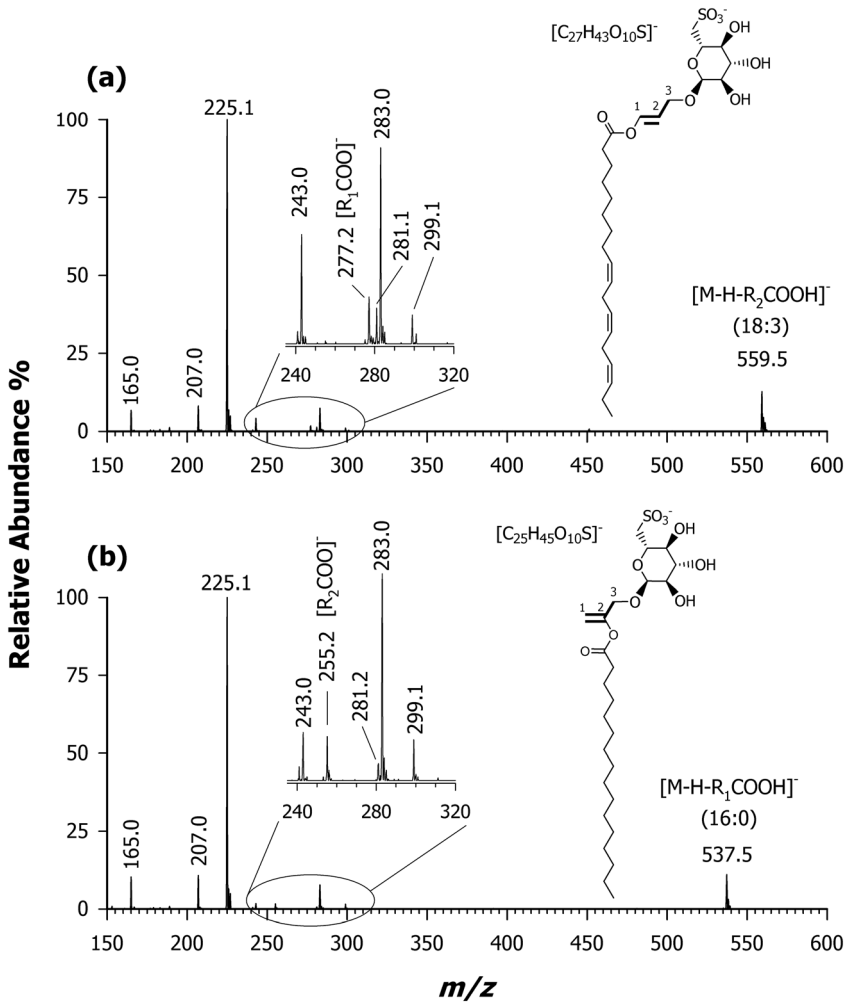

Figure 7. CID MS/MS/MS spectra of ions at *m/z* 559.5 (a) and 537.3 (b) fragmented at 30% collision energy. These precursor ions are the product ions $[M-H-R_2COOH]^-$ and $[M-H-R_1COOH]^-$, respectively, of the 18:3/16:0 SQDG at *m/z* 815.5 (see Fig. 4). See Scheme 2B for product ion assignments.

and for product ions related to the sulfoquinovosyl moiety (i.e. *m/z* 243.0, 207.0 and 165.0) are reported. While the chemical formulas, i.e. $[C_9H_{13}O_8S]^-$ and $[C_9H_{15}O_8S]^-$, seem to be consistent with literature data,[14] we speculate that the chemical structures of both ions at *m/z* 281.0 and 283 are those ones reported in the panel B of Scheme 2. We do not rule out that both these product ions would have different structures, even if these last appear enough plausible in the view of the entire fragmentation pattern observed. The *m/z* 243.0 ion ($[C_6H_{11}O_8S]^-$), which is produced from both $[M-H\ R_1COOH]^-$ and $[M-H-R_2COOH]^-$, is evidences for the generation of the monosaccharide 6-deoxy-6-sulfo-quinovopyranose as a result of glycosyl cleavages from the glycerol residue. Additional examples of MS^3 experiments performed on precursor ions $[M-H-R_1COOH]^-$ and $[M-H-R_2COOH]^-$ (ions at *m/z* 563.5 and 537.5, respectively, obtained from the 18:1/16:0 SQDG at *m/z* 819.5) are given in Fig. S3 (see Supporting Information).

The biosynthesis of SQDG species in spinach leaves

From a biosynthetic point of view, interesting considerations can be drawn from the SQDG regiochemical assignments data reported in **Table 1**, representing, to the best of our knowledge, the most extensive characterization currently available for plant sulfolipids. First, a semi-quantitative interpretation of MS data relevant to the SQDGs mixture was attempted. In particular, the peak areas obtained from the XIC traces for all the identified species were used to evaluate their distribution in the analyzed plant extract, thus assuming comparable ESI yields. The percent area values for the ten most abundant SQDGs, normalized to that of the most abundant sulfolipid 18:3/16:0 (*m/z* 815.5) are reported in **Fig. 8**.

Half of the 24 identified species bear a 16:0 acyl chain on the *sn*-2 position, and five of them are included among the ten most abundant components.[23] The nature and position of acyl chains in the SQDGs can provide useful information on their biosynthesis in higher plants, which is known to occur within plastids.[32–36] Actually, SQDG synthase can use either DAGs formed via the chloroplastic (prokaryotic) pathway or those imported from the endoplasmic reticulum (eukaryotic pathway).[37,38] DAGs originated within the chloroplasts usually bear a 18:1 acyl chain on the *sn*-1 position and a 16:0 one on the *sn*-2 position, a combination corresponding to a typical prokaryotic-type cell.[33,34] On the contrary, DAGs generated through a eukaryotic pathway usually contain a mixture of 18:2 and 18:3 side chains at both *sn*-1 and *sn*-2 positions and a 16:0 chain in the *sn*-1

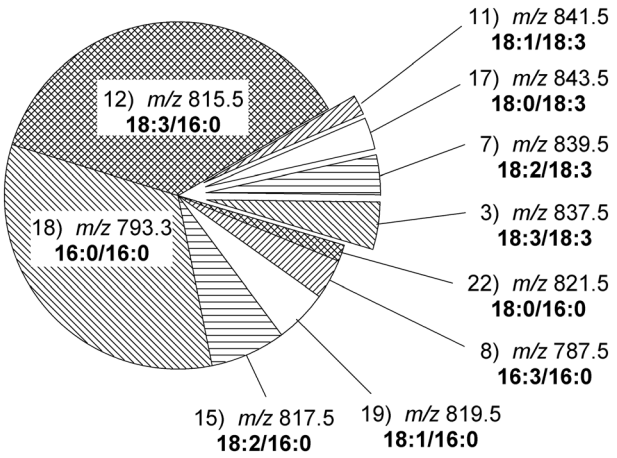

Figure 8. Pie chart representing the distribution of the ten most abundant SQDG species identified in the lipid extract of spinach leaves by LC/ESI MS and MS/MS in negative ion mode. The peak number used in Table 1, the *m/z* value and the *sn*-1/*sn*-2 regiochemistry are given for each species.

position.[33,34] The cited moieties were those actually found in the ten most abundant SQDGs identified in the present work. Consequently, the prevailing location of the 16:0 acyl chain on the *sn*-2 position of the most abundant SQDGs is in good agreement with the preferential biosynthetic path in spinach leaves, being indeed of prokaryotic-type. We envision that the proposed approach will enable the systematic investigation of plant and bacteria samples with broad implications within and beyond the realm of sulfolipids and their involvement in membrane structures and cell communication.

Conclusions

LC/ESI-MS^n (n = 1–3) in a linear ion trap allowed a full characterization of plant sulfolipids, leading to the identification of 24 different species in a lipid extract of spinach leaves. Interesting information is obtained both on their low-energy (CID) dissociations and on their biosynthetic pathways. Tandem MS of SQDG precursor ions clearly demonstrated a remarkable loss of neutral fatty acids from their side chains, clearly prevailing over ketene loss and carboxylate anion generation. This feature may be fully developed to enable recognition of structural isomers. At a more refined level of structural characterization, a systematic prevalence of fatty acid loss from the *sn*-1 position of glycerol was observed and exploited for the regiochemical *sn*-1/*sn*-2 assignment. The prevailing presence of saturated acyl chains on the *sn*-2 position of the identified SQDGs indicates a prokaryotic pathway as the main route for their biosynthesis in spinach leaves. Clearly, the present investigation opens interesting perspectives for a more extended characterization of sulfolipids having relevance in vegetal and in bacterial or algal lipidomics. However, the issue of lack of standard must be further addressed before the method can be applied in the LC/ESI-MS/MS analysis of unknown SQDGs in complex mixtures.

Acknowledgement

We wish to thank the anonymous reviewers for their valuable and insightful suggestions. We acknowledge the financial support of the Ministero dell'Università, dell'Istruzione e della Ricerca, MIUR (Italy) PRIN 2009 (2009KW27KE_003). Part of this work was performed by using the instrumental facilities of CIGAS Center founded by EU (Project n° 2915/12), Regione Basilicata and Università degli Studi della Basilicata (Potenza).

Supporting information

Additional supporting information may be found in the online version of this article.

References

[1] M. Pulfer, R. C. Murphy. Electrospray mass spectrometry of phospholipids. *Mass Spectrom. Rev.* **2003**, *22*, 332.
[2] Y. H. Kim, J. S. Yo, M. S. Kim. Structural characterization of sulfoquinovosyl, monogalactosyl and digalactosyl diacylglycerols by FAB-CID-MS/MS. *J. Mass Spectrom.* **1997**, *32*, 968.
[3] M. Herrero, M. J. Vicente, A. Cifuentes, E. Ibáñez. Characterization by high-performance liquid chromatography/electrospray ionization quadrupole time-of-flight mass spectrometry of the lipid fraction of *Spirulina platensis* pressurized ethanol extract. *Rapid Commun. Mass Spectrom.* **2007**, *21*, 1729.
[4] C. Benning. Biosynthesis and function of the sulfolipid sulfoquinovosyl diacylglycerol. *Annu. Rev. Plant Physiol. Plant Mol. Biol.* **1998**, *49*, 53.
[5] A. A. Benson, H. Daniel, R. Wiser. A sulfolipid in plants. *Proc. Natl. Acad. Sci. USA* **1959**, *45*, 1582.
[6] J. Barber, K. Gounaris. What role does sulpholipid play within the thylakoid membrane? *Photosynthesis Res.* **1986**, *9*, 239.
[7] M. Shimojima. Biosynthesis and functions of the plant sulfolipid. *Prog. Lipid Res.* **2011**, *50*, 234.
[8] U. Pick, K. Gounaris, M. Weiss, J. Barber. Tightly bound sulpholipids in chloroplast CFO-CF1. *Biochim. Biophys. Acta* **1985**, *808*, 415.
[9] K. P. Howard, J. H. Prestegard. Conformation of sulfoquinovosyldiacylglycerol bound to a magnetically oriented membrane system. *Biophys. J.* **1996**, *71*, 2573.
[10] K. R. Gustafson, J. H. Cardellina II, R. W. Fuller, O. S. Weislow, R. F. Kiser, K. M. Snader, G. M. L. Patterson, M. R. Boyd. AIDS-antiviral sulfolipids from cyanobacteria (blue-green algae). *J. Natl. Cancer Inst.* **1989**, *81*, 1254.
[11] S. Aoki, K. Ohta, T. Yamazaki, F. Sugawara, K. Sagakuchi. Mammalian mitotic centromere-associated kinesin (MCAK): A new molecular target of sulfoquinovosylacylglycerols novel antitumor and immunosuppressive agents. *FEBS J.* **2005**, *272*, 2132.
[12] K. Sakaguchi, F. Sugawara. New cancer chemotherapy agents: inhibitors of DNA polymerase. *Curr. Drug Therapy* **2008**, *3*, 44.
[13] D. A. Gage, Z. H. Huang, C. Benning. Comparison of sulfoquinovosyl diacylglycerol from spinach and the purple bacterium Rhodobacter spaeroides by fast atom bombardment tandem mass spectrometry. *Lipids* **1992**, *27*, 632.
[14] X. Zhang, C. J. Fhanera, S. M. Ferguson-Millerb, G. E. Reid. Evaluation of ion activation strategies and mechanisms for the gas-phase fragmentation of sulfoquinovosyldiacylglycerol lipids from *Rhodobacter sphaeroides*. *Int. J. Mass Spectrom.* **2012**, *316–318*, 100.
[15] M. Keusgen, J. M. Curtis, P. Thibault, J. A. Walter, A. Windust, S. W. Ayer. Sulfoquinovosyl diacylglycerols from the alga *Heterosigma carterae*. *Lipids* **1997**, *32*, 1101.
[16] I. Naumann, K. H. Darsow, C. Walter, H. A. Lange, R. Buchholz. Identification of sulfoglycolipids from the alga *Porphyridium purpureum* by matrix-assisted laser desorption/ionisation quadrupole ion trap time-of-flight mass spectrometry. *Rapid Commun. Mass Spectrom.* **2007**, *21*, 3185.
[17] J. Xu, D. Chen, X. Yan, J. Chen, C. Zhou. Global characterization of the photosynthetic glycerolipids from a marine diatom *Stephanodiscus* sp. by ultra performance liquid chromatography coupled with electrospray ionization-quadrupole-time of flight mass spectrometry. *Anal. Chim. Acta* **2010**, *663*, 60.
[18] I. Naumann, B. C. Klein, S. J. Bartel, K. H. Darsow, R. Buchholz, H. A. Lange. Identification of sulfoquinovosyldiacyglycerides from *Phaeodactylum tricornutum* by matrix-assisted laser desorption/ ionization QTrap time-of-flight hybrid mass spectrometry. *Rapid Commun. Mass Spectrom.* **2011**, *25*, 2517.
[19] X. Yan, D. Chen, J. Xu, C. Zhou. Profiles of photosynthetic glycerolipids in three strains of *Skeletonema* determined by UPLC/Q-TOF-MS. *J. Appl. Phycol.* **2011**, *23*, 271.

[20] R. Welti, X. Wang, T. D. Williams. Electrospray ionization tandem mass spectrometry scan modes for plant chloroplast lipids. *Anal. Biochem.* **2003**, *314*, 149.
[21] R. Welti, X. Wang. Lipid species profiling: a high-throughput approach to identify lipid compositional changes and determine the function of genes involved in lipid metabolism and signaling. *Curr. Opin. Plant Biol.* **2004**, *7*, 337.
[22] X. Wang, W. Li, M. Lia, R. Welti. Profiling lipid changes in plant response to low temperatures. *Physiol. Plant.* **2006**, *126*, 90.
[23] Y. Takahashi, Y. Itabashi, M. Suzuki, A. Kuksis. Determination of stereochemical configuration of the glycerol moieties in glycoglycerolipids by chiral phase high-performance liquid chromatography. *Lipids* **2001**, *36*, 741.
[24] F. -F. Hsu, J. Turk. Electrospray ionization with low-energy collisionally activated dissociation tandem mass spectrometry o glycerophospholipids: mechanisms of fragmentation and structural characterization. *J. Chromatogr. B* **2009**, *877*, 2673.
[25] G. Guella, R. Frassanito, I. Mancini. A new solution for an old problem: the regiochemical distribution of the acyl chains in galactolipids can be established by electrospray ionization tandem mass spectrometry. *Rapid Commun. Mass Spectrom.* **2003**, *17*, 1982.
[26] R. V. V. Tatituri, M. B. Brenner, J. Turk, F. -F. Hsu. Structural elucidation of diglycosyl diacylglycerol and monoglycosyl diacylglycerol from *Streptococcus pneumoniae* by multiple-stage linear ion-trap mass spectrometry with electrospray ionization. *J. Mass Spectrom.* **2012**, *47*, 115.
[27] A. P. Tulloch, E. Heinz, W. Fischer. Combination and positional distribution of fatty acids in plant sulfolipids. *Hoppe Seyler's Z. Physiol. Chem.* **1973**, *354*, 879.
[28] W. Fischer, E. Heinz, M. Zeus. The suitability of lipase from *Rhizopus arrhizus delemar* for analysis of fatty acid distribution in dihexosyl diglycerides, phospholipids and plant sulfolipids. *Hoppe Seyler's Z. Physiol. Chem.* **1973**, *354*, 1115.
[29] F. -F. Hsu, J. Turk. Electrospray ionization/tandem quadrupole mass spectrometric studies on phosphatidylcholines: the fragmentation processes. *J. Am. Soc. Mass Spectrom.* **2003**, *14*, 352.
[30] M. L. Gross. Charge-remote fragmentation: an account of research on mechanisms and applications. *Int. J. Mass Spectrom.* **2000**, *200*, 611.
[31] C. Cheng, M. L. Gross. Applications and mechanisms of charge-remote fragmentation. *Mass Spectrom. Rev.* **2000**, *19*, 398.
[32] P. Dormann, C. Benning. Galactolipids rule in seed plants. *Trends Plant Sci.* **2002**, *7*, 112.
[33] C. Benning, R. Garavito, M. Shimojima. In *Advances in Photosynthesis and Respiration, Vol 27: Sulfur metabolism in Phototrophic Organism*, R. Hell, C. Dahl, D. Knaff, T. Leustek (Eds). Springer: Dordrecht, **2008**, pp. 185–200.
[34] J. P. Williams, V. Imperial, M. U. Khan, J. N. Hodson. The role of phosphatidylcholine in fatty acid exchange and desaturation in *Brassica napus* L. leaves. *Biochem. J.* **2000**, *349*, 127.
[35] M. Frentzen. Phosphatidylglycerol and sulfoquinovosyldiacylglycerol: anionic membrane lipids and phosphate regulation. *Curr. Opin. Plant Biol.* **2004**, *7*, 270.
[36] B. Yu, C. Xu, C. Benning. *Arabidopsis* disrupted in *SQD2* encoding sulfolipid synthase is impaired in phosphate-limited growth. *Proc. Natl. Acad. Sci. USA* **2002**, *99*, 5732.
[37] R. Douce, J. Joyard. In *Advances in Photosynthesis and Respiration, Vol 4: Oxygenic photosynthesis: the Light Reactions*, D. R. Ort, C. F. Yocum (Eds). Kluwer Academic Publishers: Dordrecht, **1996**, pp. 69–101.
[38] J. Browse, C. Somerville. Glycerolipid Synthesis: Biochemistry and Regulation. *Annu. Rev. Plant Physiol. Plant Mol. Biol.* **1991**, *42*, 467.

